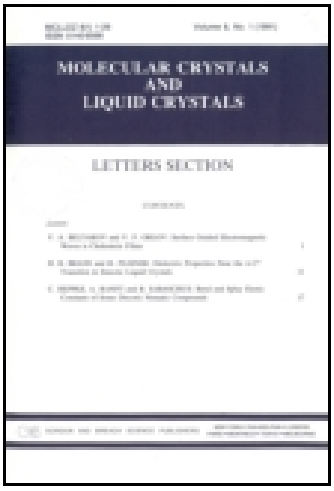

Molecular Crystals and Liquid Crystals
Publication details, including instructions for authors and subscription information:
http://www.tandfonline.com/loi/gmcl20

Effects of a Seed Layer and Sn Ion Modification on the ZnO Nanorods in Dye-Sensitized Solar Cells

Seok Cheol Choi[a] & Sang Ho Sohn[a]
[a] Department of Physics, Kyungpook National University, Daegu, Korea
Published online: 06 Dec 2014.

To cite this article: Seok Cheol Choi & Sang Ho Sohn (2014) Effects of a Seed Layer and Sn Ion Modification on the ZnO Nanorods in Dye-Sensitized Solar Cells, Molecular Crystals and Liquid Crystals, 602:1, 72-80, DOI: 10.1080/15421406.2014.944637

To link to this article: http://dx.doi.org/10.1080/15421406.2014.944637

Mol. Cryst. Liq. Cryst., Vol. 602: pp. 72–80, 2014

ISSN: 1542-1406 print/1563-5287 online
DOI: 10.1080/15421406.2014.944637

Taylor & Francis
Taylor & Francis Group

Effects of a Seed Layer and Sn Ion Modification on the ZnO Nanorods in Dye-Sensitized Solar Cells

SEOK CHEOL CHOI AND SANG HO SOHN*

Department of Physics, Kyungpook National University, Daegu, Korea

ZnO nanorods are modified by Sn ion and investigated their physical characteristics. The effects of seed layers prepared by sputtering and spin-coating methods on the FTO glasses were also studied. ZnO nanorods were synthesized by a sonochemical method using a zinc acetate dehydrate as a precursor. The Sn-doped ZnO nanorods were synthesized using a tin tetrachloride by a sonochemical method. The characteristics of well-aligned ZnO nanorods were investigated by a FE-SEM, XRD, photoluminescence (PL) with respect to two aspects such as growth methods of a seed layer and tin tetrachloride ion modifications. The Sn doping can form new band structure in the ZnO nanorods, which can effectively control their light absorption spectra and improve the energy conversion efficiency of the ZnO nanorod-based dye sensitized solar cells (DSSCs).

Keywords Ion modification; seed; dye-sensitized solar cell; ZnO nanorod; sonochemical

Introduction

Dye-sensitized solar cell (DSSC) using inorganic semiconductor is being studied as a new type of solar cell and expected as a low cost alternative to silicon-based photovoltaic solar cells [1–3].

A TiO_2 nanoparticle film has been used as a photoelectrode material in DSSCs due to its large surface area, which enables efficient light harvesting [4]. However, the TiO_2/electrolyte interface tends to affect the electro-optical properties of DSSCs such as photovoltage, photocurrent density and energy conversion efficiency [5]. Therefore, other semiconducting materials such as SnO_2 [6], Nb_2O_5 [7] and ZnO [8] have been used to enhance the photoelectrochemical properties of the DSSCs. Among these candidates, ZnO has attracted much attention because of similar band structure and electronic properties to TiO_2 [9]. Conventional methods for synthesizing the ZnO nanostructures have been based on vapor-phase reactions and a hydrothermal synthesis. However, the vapor method requires high temperatures (up to 1400°C) and low pressure. Moreover, the hydrothermal method requires much growth time, which takes from several hours to several days. Recently, a quick sonochemical method for the ZnO nanorod fabrication was reported [10]. Therefore, we synthesized the ZnO nanorod by the sonochemical method a low temperature of 90°C.

*Address correspondence to Prof. Sang Ho Sohn, Department of Physics, Kyungpook National University, Sangyuk-dong, Buk-gu, Daegu 702-701, Korea (ROK). E-mail: shsohn@knu.ac.kr

Color versions of one or more of the figures in the article can be found online at www.tandfonline.com/gmcl.

Table 1. Growth conditions of ZnO nanorods fabricated different seed growth methods with and without Sn ion modification and their physical characteristics

Samples	Seed method	Ion precursor	PL intensity ratio[a]	Adsorbed N719[b] ($mol \cdot dm^{-3}$)
A	Sputtering	—	~1.21	4.09×10^{-6}
B	Sputtering	Tin tetrachloride	~0.81	4.79×10^{-6}
C	Spin-coating	—	~0.75	5.03×10^{-6}
D	Spin-coating	Tin tetrachloride	~0.51	5.53×10^{-6}

[a]The intensity ratio is defined as the ratio of the UV peak intensity to the visible peak intensity in PL spectra as shown in Fig. 3.
[b]Adsorbed N719 was calculated from the UV-Vis absorption spectra, counting on the Beer-Lambert law as shown in Fig. 4.

In this work, ZnO nanorods were synthesized by a sonochemical method using zinc acetate dehydrate as a precursor. This study focused on two effects, such as a seed layer and Sn ion modification. A seed layer was prepared by sputtering and spin-coating methods, and Sn ion modification of the ZnO nanorods was synthesized using a tin tetrachloride as a precursor. Moreover, the investigations on the ZnO nanorods fabricated under different growth conditions on the photoelectrochemical properties in DSSC were performed.

Experimental

Preparation of Seed Layer on FTO Substrates

ZnO films with thickness of 20 nm as a seed layer were grown on the FTO substrate at room temperature by a sputtering method. The sputtering power and time were 50 W and 10 min, respectively. In addition, Zinc acetate dehydrate was dissolved in the mixed solution of ethanol, Then the solution was spin-coated onto FTO substrates at 800 rpm for 1 min. These processes repeated 6 times.

Synthesis of ZnO Nanorods with and without Sn Ion Modification

0.03M of zinc acetate dehydrate was dissolved in deionized water. Subsequently, ZnO nanorod was synthesized by a sonochemical method at 90° for 1 h. Moreover, 0.03 M of zinc acetate dehydrate was dissolved in deionized water. Subsequently, ZnO nanorod was synthesized by a sonochemical method at 90° for 1 h. In addition, Sn ion-modified ZnO nanorods were synthesized by the same sonochemical method as previously described, using zinc acetate dehydrate and tin tetrachloride, adding the latter to the former within 2 atomic percent (at%). Ultrasonication was performed by a sonochemical apparatus with a frequency of ultrasonic wave 20 kHz under ambient conditions in order to grow aligned ZnO nanorods with and without Sn ion-modification. The resultant ZnO nanorods were then washed with DI water, and dried at 70° for 1 h. Table 1 lists the growth conditions of ZnO nanorods under different seed growth method and Sn precursor to investigate their morphological and optical effects on the seed layer and Sn ion modification. Denomination

A, B, C, and D implies ZnO nanorod samples prepared under different seed growth methods and Sn ion precursor.

Fabrication of DSSC

ZnO nanorods were immersed in 0.5 mM N719 dye solution (a mixture of tert-butyl alcohol and ethanol, 1:1 by volume ratio) in dry ethanol for 3hrs and then washed by ethanol. Platinum was coated on the FTO glass by a spin coating method to obtain platinized FTO glasses used as a counter electrode. The two substrates with a dye-adsorbed photoelectrode and a Pt counter electrode each were assembled using a Surlyn film as a bonding agent. A drop of electrolyte solution (SOLARONIX, AN-50) is placed on the drilled hole in the counter electrode of the assembled cell. Finally, the hole is sealed by using a cover glass.

Growth Mechanism

The growth mechanism of the ZnO nanorods takes into consideration the radical species generated from the water molecules [11]. On the basis of the growth mechanism introduced in Ref. 11, we propose a two-step mechanism for the formation of ZnO nanorods from aqueous metal acetates that uses sonochemical oxidation and sonochemical hydrolysis (sonohydrolysis). The likely first reaction step for the sonochemical oxidation process can be summarized as follows:

$$Zn(CH_3COO)_2(s) \rightarrow Zn^{2+}(aq) + 2(CH_3COO) - (aq) \quad (1)$$

The likely next reaction step for sonohydrolysis is given by

$$Zn^{2+}(aq) + H_2O(l) \rightarrow ZnO(s) + 2H^+(aq) \quad (2)$$

The formation of the ZnO nanorods occurs at the interface of the solution bubble [12].

Measurements

The comparison and analysis of the material properties between the surface-coated and the non-coated ZnO nanorods was done by the help of FE-SEM (field emission scanning electron microscopy, HITACHI S-4800), XRD (X-ray Diffraction, X'Pert MPD), and UV-VIS-NIR (ultraviolet-visible-near infrared, Cary 5 spectrophotometer). The room-temperature photoluminescence (PL) characteristics of the ZnO nanowires on FTO glass were measured. The PL spectra were excited by using a 325 nm wavelength He-Cd Laser (30 mW) and detected by using a GaAs photomultiplier tube. I-V and IPCE characteristics of ZnO nanorod-based DSSC device with the active area of $0.5 \times 0.5 cm^2$ were measured under 100 $mWcm^{-2}$ of simulated AM 1.5 solar light by using a Solar Simulator (PEC-L12, Peccell).

Results and Discussion

Figure 1 shows the FESEM images of the cross section for ZnO nanorods grown by the sonochemical method on the sputtered seed layer and the spin-coated one with and without Sn ion modification. The hexagonal nanorods covered the entire surface of the FTO glass. We observed that the ZnO nanorods have the diameter ranging from 30 to

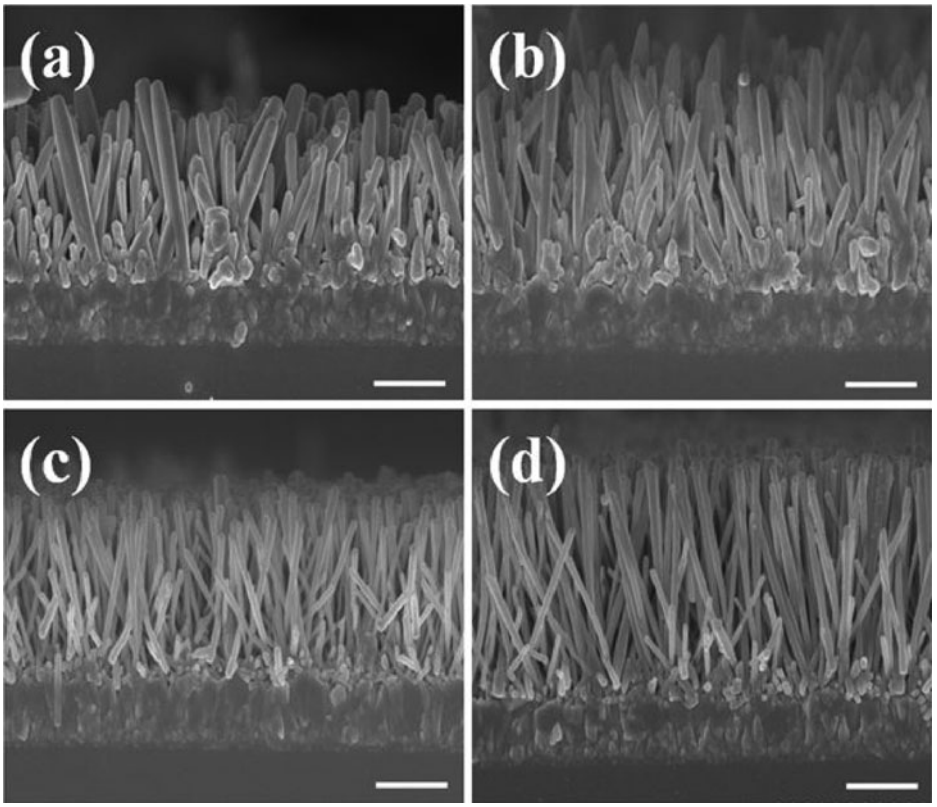

Figure 1. The FESEM images of the ZnO nanorods grown under different seed growth and Sn ion modification conditions: (a) sample A, (b) sample B, (c) sample C, and (d) sample D. The scale bar is 1μm.

100 nm and the length ranging from 1 to 4 μm, showing the preferred orientation in the c-axis direction. It is also found that the ZnO nanorods grown on the spin-coated seed layer show better morphological characteristics than that grown on the sputtered one. Moreover, Sn ion-modified ZnO nanorods display better preferred orientation and growth compared to as-grown ones, indicating that Sn ion modification leads to faster growth rate during a sonochemical synthesis than non-modification cases. We observed the changes in surface morphology of Sn ion-modified ZnO nanorods, which is due to the tin tetrachloride contained in precursor solution that used in the sonochemical synthesis.

Figure 2 show the XRD pattern of ZnO nanorods on the seed layer grown under different seed growth and ion modification conditions. The XRD results reveal that all samples have the wurtzite structure with three peaks at different 2theta of about 31.7, 34.4 and 36.2°, corresponding to the crystal planes of (100), (002) and (101) of ZnO, respectively [13]. This indicates that the Sn ion added in solutions had no effect on the crystal structure of the ZnO nanorods. There are two peaks at about 33.7° and 37.1° due to the FTO glass substrate. Also, there were no diffraction peaks observed from other impurities in the XRD patterns. The intensity of ZnO (002) plane increases in the order of A, B, C, and D samples due to the faster growth rate of ZnO nanorods by spin coating method and Sn ion modification, which matches to the SEM results as shown in Fig. 1. All samples exhibited preferentially-oriented structures with respect to the c plane. One can find that The diffraction intensity

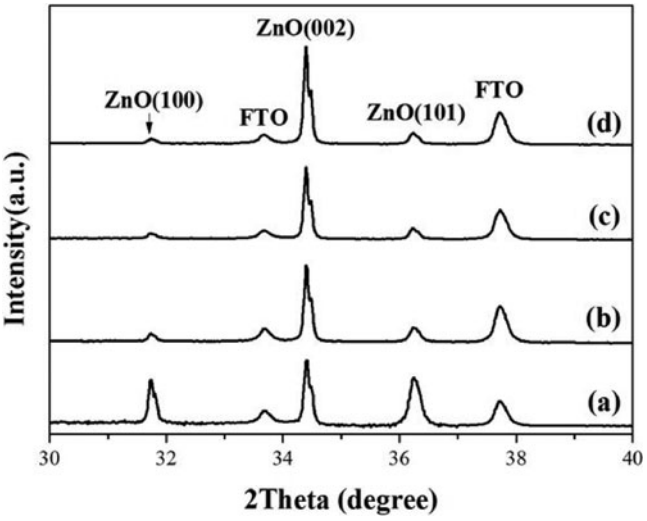

Figure 2. The XRD patterns of the ZnO nanorods grown under different seed growth and Sn ion modification conditions: (a) sample A, (b) sample B, (c) sample C, and (d) sample D.

of (002) plane of ZnO nanorods fabricated by spin coating method is higher than that of ZnO nanorods fabricated seed layer of sputtering method. Moreover, Sn ion-modified ZnO nanorods have better preferred orientation with respect to the c axis, compared to as-grown ones. In the Sn ion-modified ZnO nanorods, the peak positions at (002) plane are so similar to non-modified ones, indicating that any expected shift in lattice constant would be beyond the resolution of our XRD diffractometer. In addition to the highest (002) peak, two peaks of (100) and (101) appeared in the XRD patterns of all the samples. The diffraction peaks at (100) and (101) planes was weakly observed for the B, C, and D samples, showing that the two peak intensities for the three samples is almost same. Thus, the Sn ion-modified ZnO nanorods grown on spin-coated seed layer (sample D) exhibit strongly preferred orientation in the c-axis direction, which is due to a higher diffraction intensity of (002) plane than other samples, as seen in Fig. 2.

Figure 3 shows the normalized photoluminescence (PL) spectra of the ZnO nanorod grown under different seed growth and Sn ion modification conditions. A narrow UV band at about 3.3 eV (372 nm wavelength) and a broad green band, ranging at 2.19 eV (568 nm wavelength) were observed for all samples. The UV emission band can be explained by a near band-edge transition of the wide band gap ZnO nanorods [14]. We observed that the Sn ion-modified ZnO nanorods have broader UV peaks than as-grown ones, implying that the precursors with Sn ion cause changes in the energy band configuration of the ZnO nanorods, and thus decrease the optical properties in UV region. The green band emission resulted from the recombination of a photo-generated hole with an electron that belonged to a singly-ionized oxygen vacancy [15]. Considering the previously calculated ZnO band structure, the visible emission can be assigned to oxygen vacancy and zinc interstitial [16]. To investigate on the defects in ZnO nanorods, the UV peak intensities are normalized. Compared to the UV emission of the ZnO nanorods, the visible emission increases in the order of A, B, C, and D samples, as shown in Fig. 3 (black, red, blue, and dark cyan lines, respectively). The ZnO nanorods grown on spin-coated seed layer have better visible

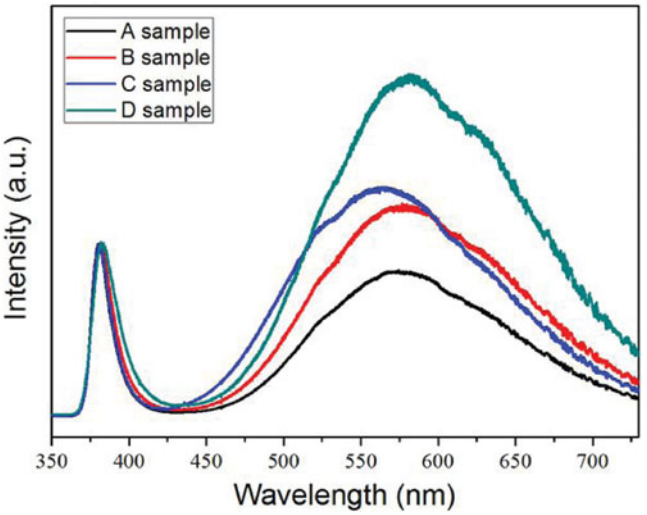

Figure 3. The normalized PL spectra of the ZnO nanorods grown under different seed growth and Sn ion modification conditions for the samples A, B, C and D.

emission than that grown on sputtered one, which is due to their enhanced preferential-oriented structures by spin coating method. It is also found that the Sn ion-modified ZnO nanorods have broader visible peaks with a redshift compared to as-grown ones, which is attributed to the increases in the oxygen vacancy and Zn interstitial by Sn ion modification. To compare these PL properties, we introduced an intensity ratio, which is defined as the ratio of the UV peak intensity to the visible peak intensity in PL spectra. The PL intensity ratios for the A, B, C, and D samples are about 1.21, 0.81, 0.75, and 0.51, respectively, as listed in Table 1. We observed that the intensity ratio decreases in the order of A, B, C, and D samples due to the enhanced visible emission, which can be applied to dye-sensitized solar cell. Therefore, we suggest that we can control the visible emission of the ZnO nanorods grown using sonochemical methods by controlling the seed growth and Sn contents.

Figure 4 shows the absorbance spectra of dyes detached from the ZnO nanorods grown under different seed growth and Sn ion modification conditions. All spectra exhibited two absorption bands at about 375 and 515 nm, which indicates the characteristics of N719 dye [17]. The spectra show that the absorbance increases in the order of A, B, C, and D samples. This fact is due to the changes in the specific surface area, yielding changes in dye loading. To estimate the adsorbed amount of dye for four samples A∼D, we used on the Beer-Lambert law. A rearranged form of the Beer-Lambert law for the ZnO nanorods allowed us to calculate the number of moles of dye adsorbed on the surface of the ZnO using the following equation:

$$A = a \cdot b \cdot C \tag{3}$$

where A is the absorbance, a is the molar extinction coefficient of the dye in solution ($M^{-1} \cdot cm^{-1}$), b is the path length (cm), and C is the concentration of the sample solution (M). The UV-vis absorption spectra of the resultant solution, whose molar extinction coefficient was determined to be 1.41×10^4 dm^3 mol^{-1} cm^{-1} at 515 nm [18], were measured using a 1 cm quartz cell to estimate the adsorbed amount of dye. Using the given values $a = 1.41 \times 10^4$ dm^3 mol^{-1} cm^{-1} at 515 nm, $b = 1$ cm, and the A values measured at 515 nm, we

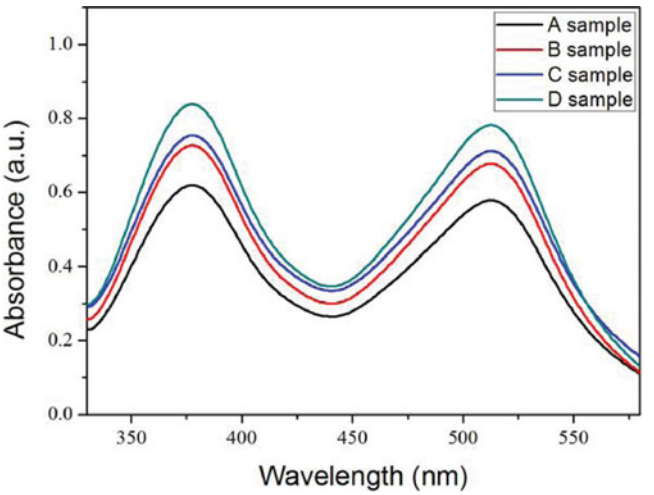

Figure 4. Absorbance spectra of dyes detached from the ZnO nanowires grown under different seed growth and Sn ion modification conditions for the samples A, B, C and D.

can calculate concentration C using Eq. 3. As listed in Table 1, the adsorbed dye amounts were calculated for the four samples and the calculated results indicate that the dye amount increases in the order of A, B, C, and D samples, which is attributed to the enhanced specific surface area due to the increase in aspect ratios.

Figure 5 shows photocurrent density (I) vs. photovoltage (V) curves of the DSSCs fabricated by using ZnO nanorods grown under different seed growth and Sn ion modification conditions. The I-V curves show that the electro-optical characteristics of DSSC devices increase in the order of sample A, B, C, and D. This result seems to originate from the enhanced dye loading, as shown in Fig. 4 and Table 1.

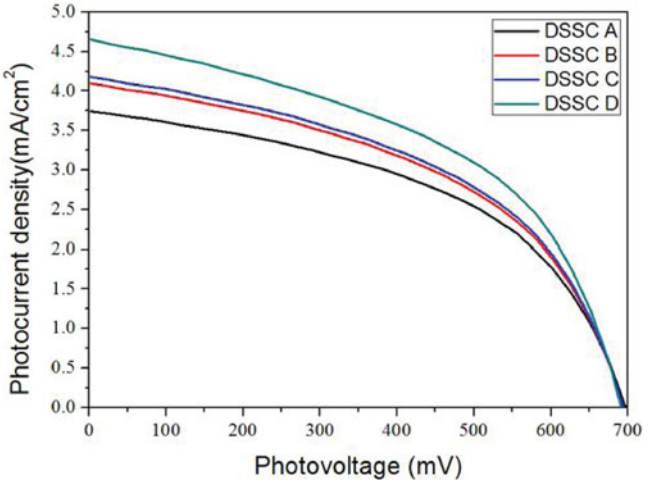

Figure 5. I-V characteristics of DSSC devices fabricated using ZnO nanowires grown under different seed growth and Sn ion modification conditions (DSSC A, B, C and D).

Table 2. Electro-optical characteristics of DSSCs with ZnO nanorods

DSSC devices[a]	ZnO photoelectrodes	V_{oc} (mV)	J_{sc} (mA/cm^2)	FF (%)	Efficiency (%)
DSSC A	Sample A	697.1	3.75	52.4	1.37
DSSC B	Sample B	693.1	4.10	52.0	1.48
DSSC C	Sample C	693.2	4.18	52.3	1.52
DSSC D	Sample D	690.8	4.65	52.7	1.69

[a]Cells were measured under 100 mWcm^{-2} of simulated AM 1.5 solar light.

Table 2 lists the electro-optical characteristics of DSSCs fabricated using ZnO nanorods grown under different seed growth and Sn ion modification conditions. A maximum efficiency of 1.69% was achieved in the case of DSSC D with short-circuit photocurrent density (J_{sc}) = 4.65 mA/cm^2, open-circuit photovoltage (V_{oc}) = 690.8 mV, and fill factor (FF) = 52.7%. Enhanced energy conversion efficiency results largely from an increased value of J_{sc}. There are no changes in V_{oc}, indicating that the ZnO nanorods have no changes in Fermi level by Sn ion modification, which matches to XRD and PL shown in Figs. 2 and 3, respectively.

Figure 6 shows IPCE results for DSSC devices (A∼D) fabricated using the ZnO nanorods grown under different seed growth and Sn ion modification conditions. The IPCE value increased in the order of DSSC A, DSSC B, DSSC C, and DSSC D. IPCE describes the photocurrent collected per incident photon flux as a function of illumination wavelength and it means the maximum possible efficiency with which incoming radiation can convert to electrons by the dye [19, 20]. We note that IPCE values of DSSC A and DSSC C more decreased, compared to other DSSC devices ranging from 580 to 750 nm in wavelength. This result indicates that the Sn ion modifications produced an enhanced IPCE value in the long wavelength visible region. This can be explained by photoluminescence (PL) and

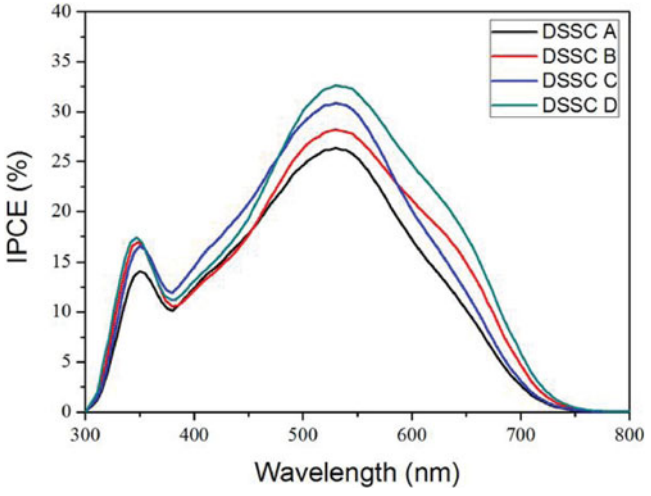

Figure 6. IPCE spectra of DSSC devices fabricated using ZnO nanowires grown under different seed growth and Sn ion modification conditions (DSSC A, B, C and D).

light scattering processes in the ZnO nanorods as follows. Once a Sn ion enters the ZnO lattice, a defect energy level is formed in ZnO energy band structures. Electrons excited by solar energy are trapped at the defect levels, and then the electrons are deexcited by relaxing toward the valence band of ZnO. These PL processes enable to emit photons with long wavelengths in visible regions, resulting in an increase in dye sensitization, which matches to the IPCE results.

Conclusions

We investigated the effects on seed growth methods and Sn ion modifications for the ZnO nanorods in DSSCs. The Sn ion-modified ZnO nanorods grown on spin-coated seed display better vertically-preferential orientation and growth, compared to bare ZnO nanorods grown on sputtered one, resulting in the enhanced aspec ratio of the ZnO nanorods. The PL results tell that the Sn ion-modified ZnO nanorods grown on spin-coated seed have more broadening and intense in visible emission than as-grown ones, which can be applied to widening of light absorption band. This fact leads to the increases in absorbance of dye due to the changes in the specific surface area. The IPCE results showed the broadening photoluminescence effects of Sn ion-modified ZnO nanowires grown on spin-coated seed in visible bands, resulting in the enhanced I-V properties. Thus, we suggest that suitable seed and Sn ion modification yield high-quality ZnO nanorods, which can be applied to photoelectrodes in dye-sensitized solar cell.

References

[1] O'Regan, B., & Gratzel, M. (1991). *Nature*, *353*, 737.
[2] Huang, M. H., Mao, S., Feick, H., Yan, H., Wu, Y., Kind, H., Weber, E., Russo, R., & Yang, P. (2001). *Science*, *292*, 1897.
[3] Satoh, M., Tanaka, N., Ueda, Y., Ohshio, S., & Saitoh, H. (1999). *Jpn. J. Appl.Phys.*, *38*, L586.
[4] Huh, P., & Kim, S. C. (2012). *Electron. Mater. Lett.*, *8*, 131.
[5] Prakash, T. (2012). *Electron. Mater. Lett.*, *8*, 231.
[6] Katoh, R., Furube, A., Yoshihara, T., Hara, K., Fujihashi, G., Takano, S., Murata, S., Arakawa, H., & Tachiya, M. (2004). *J. Phys. Chem. B*, *108*, 4818.
[7] Sayama, K., Sugihara, H., & Arakawa, H. (1998). *Chem. Mater.*, *10*, 3825.
[8] Du Pasquier, A., Chen, H. H., & Lu, Y. C. (2006). *Appl. Phys. Lett.*, *89*, 253513–1.
[9] Chou, T. P., Zhang, Q. F., Fryxell, G. E., & Cao, G. Z. (2007). *Adv. Mater.*, *19*, 2588.
[10] Jung, S. H., Oh, E., Lee, K. H., Park, W., & Jeong, S. H. (2007). *Adv. Mater.*, *19*, 749.
[11] Vijaya Kumar, R., Diamant, Y., & Gedanken, A. (2000). *Chem. Mater.*, *12*, 2301.
[12] Jung, S. H., Oh, E. J., Lee, K. H., Park, W., & Jeong, S. H. (2007). *Adv. Mater.*, *19*, 749.
[13] Choi, S. C., Lee, H. S., & Sohn, S. H. (2012). *J. Nanosci. Nanotechnol.*, *12*, 6080.
[14] Kong, Y. C., Yu, D. P., Zhang, B., Fang, W., & Feng, S. Q. (2001). *Appl. Phys. Lett.*, *78*, 407.
[15] Vanheusden, K., Warren, W. L., Seager, C. H., Tallant, D. K., Voigt, J. A., & Gnade, B. E. (1996). *J. Appl. Phys.*, *79*, 7983.
[16] Liu, X., Wu, X., Cao, H., & Chang, R. P. H. (2004). *J. Appl. Phys. 95*, 3141.
[17] Nazeeruddin, M. K., Kay, A., Rodicio, I., Humphry-Baker, R., Muller, E., Liska, P., Vlachopoulos, N., & Gratzel, M. (1993). *J. Am. Chem. Soc.*, *115*, 6382.
[18] Wang, Z. S., Kawauchi, H., Kashima, T., & Arakawa, H. (2004). *Coord. Chem. Rev.*, *248*, 1381.
[19] Chen, Z., Jaramillo, A. J., Kleiman-Shwarsctein, A., Forman, A. J., & Garland, R. (2010). *J. Mater. Res.*, *25*, 3.
[20] Li, L., Gibson, E. A., Qin, P., Boschloo, G., Gorlov, M., Hagfeldt, A., & Sun, L. (2010). *Adv. Mater.*, *22*, 1759.